Polydatin, a potential NOX5 agonist, synergistically enhances antitumor activity of cisplatin by stimulating oxidative stress in non-small cell lung cancer

SIYUAN WU[1,2*], QI ZHAO[1,2*], SHENGJUAN LIU[1,2], JIAYANG KUANG[2], JI ZHANG[2], ANNABETH ONGA[2], YIWEI SHEN[2], JIAYING WANG[2], HEHUAN SUI[2], LIANLI NI[2], YUXIN YE[2], XINYUE TU[2], HAN-BO LE[1], YIHU ZHENG[3], RI CUI[1,2] and WANGYU ZHU[1,2]

[1]Cellular and Molecular Biology Laboratory, Affiliated Zhoushan Hospital of Wenzhou Medical University, Zhoushan, Zhejiang 316020, P.R. China; [2]Cancer and Anticancer Drug Research Center, School of Pharmaceutical Sciences, Wenzhou Medical University, Wenzhou, Zhejiang 325035, P.R. China; [3]Department of General Surgery, The First Affiliated Hospital of Wenzhou Medical University, Wenzhou, Zhejiang 325000, P.R. China

Received November 9, 2023; Accepted May 10, 2024

DOI: 10.3892/ijo.2024.5665

Abstract. Non-small cell lung cancer (NSCLC) is one of the major causes of cancer-related death worldwide. Cisplatin is a front-line chemotherapeutic agent in NSCLC. Nevertheless, subsequent harsh side effects and drug resistance limit its further clinical application. Polydatin (PD) induces apoptosis in various cancer cells by generating reactive oxygen species (ROS). However, underlying molecular mechanisms of PD and its effects on cisplatin-mediated antitumor activity in NSCLC remains unknown. MTT, colony formation, wound healing analyses and flow cytometry was employed to investigate the cell phenotypic changes and ROS generation. Relative gene and protein expressions were evaluated by reverse transcription-quantitative PCR and western blot analyses. The antitumor effects of PD, cisplatin and their combination were evaluated by mouse xenograft model. In the present study, it was found that PD in combination with cisplatin synergistically enhances the antitumor activity in NSCLC by stimulating ROS-mediated endoplasmic reticulum stress, and the C-Jun-amino-terminal kinase and p38 mitogen-activated protein kinase signaling pathways. PD treatment elevated ROS generation by promoting expression of NADPH oxidase 5 (NOX5), and NOX5 knockdown attenuated ROS-mediated cytotoxicity of PD in NSCLC cells. Mice xenograft model further confirmed the synergistic antitumor efficacy of combined therapy with PD and cisplatin. The present study exhibited a superior therapeutic strategy for some patients with NSCLC by combining PD and cisplatin.

Correspondence to: Professor Ri Cui, Cancer and Anticancer Drug Research Center, School of Pharmaceutical Sciences, Wenzhou Medical University, Building 11, Chashan Street, University Town, Wenzhou, Zhejiang 325035, P.R. China
E-mail: wzmucuiri@163.com

Dr Wangyu Zhu, Cellular and Molecular Biology Laboratory, Affiliated Zhoushan Hospital of Wenzhou Medical University, 739 Dingshen Road, Zhoushan, Zhejiang 316020, P.R. China
E-mail: zhuwangyu24@sina.cn

*Contributed equally

Key words: non-small cell lung cancer, polydatin, cisplatin, reactive oxygen species, NAPDH oxidase 5, endoplasmic reticulum stress

Introduction

Non-small cell lung cancer (NSCLC) is one of the most common malignant tumors, and the leading cause of cancer-related death worldwide (1). NSCLC accounts for ~85% of all lung cancer, including adenocarcinoma, giant cell carcinoma and squamous cell carcinoma (2). Despite significant progress in early detection and treatment strategies, the prognosis of patients with NSCLC remains poor with a 5-year overall survival rate of ~20% (3). Tumor recurrence, metastasis and drug resistance lead to treatment failure and are the main cause of NSCLC-related death (4). Thus, thorough understanding of the molecular mechanism of NSCLC progression and metastasis is urgently needed, so as to find novel therapeutic targets.

Cisplatin is a front line regimen for the treatment of NSCLC and platinum-based regimens have reported significantly improved survival outcome in patients with advanced NSCLC (5). Accumulating evidences have demonstrated that cisplatin in combination with other chemotherapeutic agents exerted stronger therapeutic efficacy than single agent alone against NSCLC. Combined treatment with olaparib (PARP inhibitor) and cisplatin exerted synergistic antitumor effects on PTEN-deficient NSCLC cells by suppressing DNA repair (6). Additionally, combinational treatment with falnidamol (EGFR inhibitor) and cisplatin remarkably induced G2/M cell cycle arrest, DNA damage and ferroptosis in NSCLC cells (7). Solamargine, a steroidal alkaloid glycoside, in combination with cisplatin induced G0/G1-phase arrest and apoptosis in

lung cancer cell lines by suppressing the hedgehog pathway (8). Combined therapy with arsenic trioxide and cisplatin exerted synergistic anti-NSCLC effects, and these effects were partly due to the induction of the caspase-independent apoptosis pathway (9). Cisplatin has been reported to exert cytotoxicity by inducing oxidative stress through increasing production of reactive oxygen species (ROS) (10). Additionally, cisplatin impacted on mitochondria and induced high level of mitochondrial ROS that led to ovarian cancer cells' death (11). However, clinical application of cisplatin in NSCLC has been limited due to its substantial side effects and drug resistance (12). Therefore, it is important to develop an effective combined therapeutic strategy that reduces cytotoxicity and enhances antitumor activity of chemotherapeutic agents including cisplatin.

Natural products from various traditional Chinese medicinal herbs have been reported to have a promising antitumor activity with low cytotoxicity. Jiyuan oridonin A exhibited antitumor activity by inducing ferroptosis through inhibiting GPX4 and accumulating ROS generation in gastric cancer cells (13). Cardamonin treatment elevated ROS levels in breast cancer cells by repressing HIF-1α-dependent metabolic reprogramming (14). A curcumin derivative, WZ35, induced ROS generation and subsequent YAP-mediated C-Jun-amino-terminal kinase (JNK) activation in breast cancer cells (15). Additionally, dihydroartemisinin potentiated the antitumor activity of oxaliplatin in colorectal cancer cells by inducing endoplasmic reticulum (ER) stress through inhibiting expression of PRDX2 (16).

Polydatin (3,40,5-Trihydroxystibene-3-β-Mono-D-Glucoside; PD) is a biologically active compound derived from the annual plant species *Polygonum cuspidatum* (17). PD has been reported to exert antitumor effects in various cancers. For instance, PD suppressed ovarian cancer cell viability by inducing apoptosis (18). In breast cancer, PD induced cell apoptosis by inhibiting Creb phosphorylation (19). Additionally, PD activated autophagy and induced apoptosis in human osteosarcoma cells by inhibiting the STAT3 signaling pathway (20). Combined treatment of osteosarcoma cells with PD and paclitaxel enhanced antitumor activity when compared with single treatment alone (21). Moreover, PD in combination with sunitinib markedly enhanced the antitumor activity by decreasing pro-inflammatory cytokines and NLRP3 inflammasome expression levels (22). However, underlying molecular mechanisms of PD and its effects on anti-NSCLC activity of cisplatin are largely unknown.

NADPH (nicotinamide adenine dinucleotide phosphate) oxidase, NOXs, is a family including seven members [NOX1 to NOX5, dual oxidase 1 (DUOX1) and DUOX2] whose primary function to generate ROS (23). Accumulating evidences suggested that NOXs exerted antitumor activities through generating ROS production in various cancers. Dihydrotanshinone (DHTS)-mediated activation of NOX5 promoted production of ROS and inhibited the IL-6/Stat3 pathway, resulting in inhibiting formation of breast cancer stem cells (CSCs) (24). Anlotinib, a multi-tyrosine kinase inhibitor, upregulated expression of NOX5 and production of ROS, and impaired mitochondrial respiration, resulting in promoting apoptosis in oral squamous cell carcinoma (25). Nevertheless, whether PD activates NOX5 function to facilitate ROS-mediated downstream signaling pathways in lung cancer remains largely unknown.

In the present study, the therapeutic efficacy of combined treatment with PD and cisplatin in NSCLC was comprehensively investigated. It was identified that PD exerts anti-NSCLC activity by increasing ROS production through promoting NOX5 expression. Moreover, PD enhanced anti-NSCLC effects of cisplatin by activating ROS-mediated ER stress, and the JNK and p38 mitogen-activated protein kinase (MAPK) signaling pathways. Taken together, the current results provide a valuable foundation for further clinical development of the combination therapy for the treatment of NSCLC.

Materials and methods

Cell culture. Human NSCLC cell lines (H1299 and H460) and human normal lung epithelial cells (BEAS-2B) were purchased from the Institute of Biochemistry and Cell Biology, Chinese Academy of Sciences. The cells were cultured routinely in RPMI-1640 medium (Gibco; Thermo Fisher Scientific, Inc.) containing 10% fetal bovine serum (FBS; Gibco; Thermo Fisher Scientific, Inc.) in a 5% CO_2 atmosphere at 37˚C. Normal human liver cells (MIHA) were purchased from the Cell Bank of Chinese Academy of Sciences, and human umbilical vein endothelial cells (HUVEC) were obtained from the American Type Culture Collection (cat. no. CRL-1730), which were cultured in F-12K medium supplemented with 10% FBS and endothelial cell growth supplement at 37˚C in a humidified cell incubator with a supply of 5% CO_2.

Chemicals and reagents. Cisplatin was obtained from TargetMol, PD was purchased from Selleck Chemicals (purity: >97%), carboplatin was obtained from MedChemExpress and N-Acetyl-l-Cysteine (NAC) was provided from Sigma Aldrich; Merck KGaA. 3-(4,5-dimethyl thiazol-2-yl) 2,5-diphenyl tetrazolium bromide (MTT) was purchased from Beijing Solarbio Science & Technology Co., Ltd. ROS probe 2',7'-dichlorodihydrofluorescin diacetate (DCFH-DA) and H&E staining kit were supplied from Beyotime Institute of Biotechnology. Antibodies against activating transcription factor 4 (ATF4; cat. no. 11815S), eukaryotic initiation factor 2 (eIF2α; cat. no. 9722S), phosphorylated eIF2α (p-eIF2α; cat. no. 3398S), cleaved-Caspase3 (cat. no. 9664S), Caspase3 (cat. no. 9662S), JNK (cat. no. 9252T), p-JNK (cat. no. 4668S), p38 MAPK (cat. no. 9212S), p-p38 MAPK (cat. no. 9211S), GAPGH (cat. no. 5174S), HRP-linked anti-rat IgG antibody (cat. no. 7077S) and HRP-linked anti-mouse IgG antibody (cat. no. 7076S) were purchased from Cell Signaling Technology, Inc. Ki-67 (cat. no. ab16667) was purchased from Abcam. NOX5 (cat. no. 25,350-1-AP), Vinculin (cat. no. 66,305-1-Ig) and Bcl-2 (cat. no. 60,178-1-Ig) antibodies were purchased from Proteintech Group, Inc.

Cell viability assay. The MTT assay was employed to assess the effects of PD, cisplatin and their combination on cell viability. In 96-well plates, H1299 and H460 cells were seeded at a density of $3x10^3$ or $5x10^3$ cells per well, respectively, and allowed to adhere for 24 h. BEAS-2B, MIHA and HUVEC cells were seeded at a density of $3x10^3$ per well and incubated for 24 h. The cells were treated with various concentrations of

PD (0, 100, 200, 300, 400, 500 and 600 μM) for 72 h. For the combined treatment, the cells were treated with PD, cisplatin or their combination at indicated concentrations for 72 h. After the completion of the incubation period, 25 μl of MTT reagent was added to each well and allowed to incubate for an additional 3 h. Subsequently, 150 μl of DMSO was added to each well to dissolve the formazan product. The absorbance of each sample was measured at a wavelength of 490 nm using a SpectraMax iD3 instrument (Molecular Devices, LLC). The Logit approach was used to evaluate the IC_{50} values. The CompuSyn 2.0 software (http://www.combosyn.com/index.html) was utilized to compute the combination index (CI) to evaluate drug interactions. It is noteworthy that a CI value of 1 signifies an additive effect when two agents are combined, while a CI >1 or CI <1 indicates an antagonistic or synergistic interaction, respectively.

Colony formation assay. The cells were seeded at a density of $2x10^3$ cells per well in 6-well plates and were allowed to adhere in 5% CO_2 atmosphere at 37˚C overnight. Subsequently, the cells were subjected to treatment with varying concentrations of PD (0, 25, 50 and 100 μM for H1299 cells and 0, 200, 400, 800 μM for H460 cells) for 72 h. For the combination therapy, the cells were treated with cisplatin (1.5 μM), PD (25 μM for H1299 cells and 500 μM for H460 cells), or their combination with or without 5 mM NAC pre-treatment for 2 h. After 7-10 days incubation, the colonies were subjected to a washing procedure using phosphate-buffered saline (PBS). Subsequently, a fixative solution consisting of 4% paraformaldehyde (PFA) was applied for a duration of 15 min at room temperature. Following fixation, 0.5% Gentian violet staining was performed for a period of 10 min at room temperature (RT). ImageJ software (version 1.53t; National Institutes of Health) was used to quantify colonies (consisting of >50 cells).

Wound healing assay. Wound healing analysis was employed to assess the capability of cell motility. The H1299 NSCLC cells were seeded into 6-well plates at a density of $3x10^5$, cultured with RPMI-1640 medium containing 2% FBS, and allowed to reach confluent monolayers. Then multiple lines were drawn in the cell monolayers with a bacteria-free 10 μl pipette tip to create wound area. The scratched cells were then removed from the plates by washing with PBS. H1299 cells were treated with cisplatin (1.5 μM), PD (20 μM), or a combination of both, with or without 5 mM NAC pretreatment for 1.5 h. Following a 48-h incubation period, the old medium was replaced with fresh RPMI-1640 medium supplemented with 2% FBS. The evaluation of the combined treatment on cell migration was performed by capturing images at the point when the wound in the control group had healed virtually or completely. The results of this assay were analyzed to determine the effects of the combined treatment on cell migration.

Measurement of ROS generation. In order to measure intracellular ROS generation, the cells were treated with the ROS-sensitive dye (DCFH-DA), and analyzed using flow cytometry. Specifically, the NSCLC cells were seeded into 6-well plates and cultured overnight in standard culture medium. The cells were exposed to PD (500 μM) for 3, 6, 9, 12 and 15 h. For combination treatment, the cells were exposed with cisplatin (60 μM for H1299 and 50 μM for H460), PD (500 μM), or a combination of both for a duration of 12 h. In the case of the combination group, NAC pretreatment was conducted at a concentration of 5 mM for a duration of 1.5 h prior to treatment. Following treatment, the cells were stained with 10 μM DCFH-DA and incubated at 37˚C in the absence of light for a period of 30 min. The ROS production (DCF fluorescence) was measured by flow cytometry using FACS Calibur (BD Biosciences), and data was analyzed using the FlowJo software (Tree Star, Inc.).

Protein extraction and western blotting. The homogenization of cells or tumor tissues was accomplished by using protein RIPA lysis buffer (cat. no. AR0103-100, Boster Biological Technology). Subsequently, lysates were subjected to centrifugation at 4˚C for 15 min at 13,400 x g to remove any undissolved debris. The Bradford protein assay kit (Bio-Rad Laboratories, Inc.) was used to measure the concentrations of total proteins extracted from cells or tumor tissues. The equal amount of protein (60 μg) and loading buffer were mixed, and separated by using a 10-12% SDS-PAGE. Then the proteins were transferred to PVDF membranes, and blocked with 5% fresh non-fat milk in TBST containing 0.1% Tween 20 for 2 h at RT. The membranes underwent incubation with the primary antibodies specific to the experiments overnight at 4˚C, which were ATF4 (1:1,000), eIF2α (1:1,000), p-eIF2α (1:1,000), cleaved-Caspase3 (1:1,000), Caspase3 (1:1,000), JNK (1:1,000), p-JNK (1:1,000), p38 MAPK (1:1,000), p-p38 MAPK (1:1,000), GAPGH (1:10,000), NOX5 (1:1,000), Vinculin (1:5,000) and Bcl-2 (1:2,000). Subsequently, the membranes were subjected to three wash cycles using TBST to remove any unbound antibodies. After washing, the membranes underwent further incubation with corresponding horseradish peroxidase-conjugated secondary antibodies [HRP-linked anti-rat IgG antibody (1:4,000) and HRP-linked anti-mouse IgG antibody (1:4,000)] for 1 h at RT. The ECL detection kit was used to detect immunoreactivity (Bio-Rad Laboratories, Inc.). ImageJ software (version 1.53t; National Institutes of Health) was used to conduct densitometric measurements.

In vivo mice xenograft model. Athymic BALB/c female nude mice (age, 5 weeks-old; weight, 18-20 g; n=25) were purchased from the Vital River Experimental Animal Center. All animal experiments were carried out in accordance with the Wenzhou Medical University's Institutional Animal Care and Use Committee (IACUC) guidelines (approval no. xmsq2022-0602; Wenzhou, China). The mice were maintained under specific pathogen-free conditions with stable RT (20-25˚C) and humidity (50-60%), following a 12-h light/dark cycle, and provided with a standard rodent diet and water *ad libitum*. The $2.5x10^6$ H460 cells per 100 μl of PBS/Matrigel mixture (1:1) were subcutaneously injected into the flanks of nude mice. The mice were divided into five experimental groups (n=5) when the tumor volumes reached to ~100 mm^3. The tumor bearing mice were intraperitoneally administered 2 mg/kg cisplatin every three days, 50 mg/kg PD every two days, or their combination for two weeks. The control group was administered vehicle only, and ROS inhibitor (NAC) was administered in drinking water (0.5 g/l) for the combination group. The health and behavior of the mice were monitored

daily, and tumor length (L), width (W) and mouse weight were measured every 2 days after treatment. The tumor volume was calculated using the following formula: $V=1/2 \times L \times W^2$. When the tumors reached nearly 15 mm in diameter on day 24, all the mice were sacrificed. No mice reached humane endpoints at the end of the experiments, defined as either losing 20% of body weight or exhibiting moribund behavior. At the experimental endpoint, all mice were euthanized by intraperitoneal injection of pentobarbital sodium (150 mg/kg) followed by cervical dislocation. The confirmation of mouse death was further verified by visually inspecting for cardiac and respiratory arrest. The tumor tissues were excised and weighed for further investigation. Histological examination of certain essential organs, including the heart, liver, kidney and lung were evaluated by using hematoxylin and eosin (H&E) staining.

Immunohistochemical (IHC) staining. The tumor tissue samples were fixed with 4% PFA for 24 h at room temperature and then embedded in paraffin. The paraffin blocks were sliced in 5-μm-thick sections and deparaffinized in xylene (Changshu Chemicals Co., Ltd.) and dehydrated with an ethanol gradient. Endogenous peroxidase activity was blocked by incubation with 3% H_2O_2 in methanol at room temperature for 15 min. The IHC was carried out according to the routine procedure. Specifically, the tumor sections were subjected to overnight incubation at 4˚C with a primary antibody targeting Ki-67 (1:100), followed by subsequent incubation with HRP-linked anti-rat IgG antibody (1:1,000) for 1 h at ambient temperature. Detection of the targeted antigen was achieved through employment of 3,3'-diaminobenzidine (DAB) for color detection. The histological investigation and potential toxicity assessment were carried out by H&E staining (hematoxylin for 5 min and 0.5% eosin for 1-3 min) at room temperature with heart, liver, kidney and lung tissues. The immunostained sections were observed using a confocal microscope (magnification, x200; Leica Microsystems GmbH).

Gene knockdown experiments. H1299 cells ($3x10^5$ per well) or H460 cells ($5x10^5$ per well) were seeded in 6-well plates and incubated for 24 h at 37˚C. The NOX5 small interfering (si)RNA (Shanghai GenePharma Co., Ltd.) or non-targeting control siRNA were transfected into the cells with final concentration of 30 nM using lipofectamine 3000 reagent (Invitrogen; Thermo Fisher Scientific, Inc.), and incubated for 24 h at 37˚C. Following incubation, the cells were treated with various concentrations of PD for different time-intervals according to experimental requirement. The effectiveness of knockdown was evaluated via western blotting and reverse transcription-quantitative PCR (RT-qPCR), and the siRNA sequences are provided in Table SI. This methodology is in accordance with established academic protocols for transfecting cells and evaluating knockdown efficacy.

RT-qPCR. Total RNAs were extracted by TRIzol® reagent (Invitrogen; Thermo Fisher Scientific, Inc.) according to the manufacturer's protocol. For cDNA synthesis, 1 μg of total RNA was reverse transcribed using PrimeScript RT Master Mix (cat. no. RR036A; Takara Biotechnology Co., Ltd.) in accordance with the manufacturer's protocol. RT-qPCR was performed by using TB Green Premix Ex Taq II reagent (cat. no. RR820A; Takara) according to the manufacturer's protocol. Briefly, initial denaturation was 30 sec at 95˚C, followed by 40 cycles of denaturation (5 sec at 95˚C), annealing (34 sec at 60˚C) and extension (10 sec at 95˚C). The relative gene expression was determined using the $2^{-\Delta\Delta Cq}$ method (26), and GAPDH was used as an internal control. The primer sequences utilized for the gene amplification are provided in Table SII.

Statistical analysis. All experiments were performed in triplicate (n=3). The resulting data was presented as the mean ± standard deviation (SD), and analyzed using GraphPad Prism 8.0 software (Dotmatics). Statistical analysis was conducted using two-sample t-tests for comparison between two groups, or one-way ANOVA with Tukey's multiple comparisons test for comparison between multiple groups. $P<0.05$ was considered to indicate a statistically significant difference.

Results

PD induces cytotoxicity in NSCLC cells. Previous studies have reported that PD exerted cytotoxicity in various tumor cells with IC_{50} values ranging from 200 to 500 μM (27-29). To investigate the function of PD on NSCLC cell proliferation, H1299 and H460 cells were treated with varying dosages of PD for 72 h. The chemical structure of PD (PubChem CID: 5281718) is demonstrated in Fig. S1A. As revealed in Fig. 1A and B, PD significantly suppressed both NSCLC cell proliferation in a concentration-dependent manner with IC_{50} values of ~500 μM. Additionally, the same experiments were conducted in normal human cells. As expected, PD showed less cytotoxicity against BEAS-2B (Fig. S1B), MIHA (Fig. S1C) and HUVEC (Fig. S1D) cells when compared with NSCLC cells. In detail, 600 μM PD inhibited normal human cell proliferation only ~20% when compared with non-PD treatment group. Colony formation assay further identified that PD significantly reduced colony forming ability of both H1299 (Fig. 1C) and H460 (Fig. 1D) cells.

The effects of PD on NSCLC cell apoptosis were further investigated. High doses of PD markedly reduced the expression level of the anti-apoptotic protein Bcl-2, while increased the expression of the pro-apoptotic protein Cleaved-Caspase3 in both H1299 and H460 cells (Fig. 1E and F). These results suggested that the inhibition of cell proliferation caused by PD might partly be due to PD-induced apoptotic pathway in NSCLC.

PD activates ROS-dependent ER stress pathway in NSCLC cells. PD has been revealed to have antitumor properties by generating ROS (30). Abundant ROS production stimulates oxidative stress, resulting in cancer cell death (31). To determine whether inhibition of NSCLC cell proliferation caused by PD is associated with the increased ROS generation, H1299 and H460 cells were treated with PD, followed by incubation with DCFH-DA. Treatment of both cell lines with PD elevated fluorescence intensity in a time-dependent manner, suggesting that PD treatment boosted ROS production (Fig. 2A and B). Increased ROS production triggers the ER stress response and promotes the expression levels of p-eIF2α and ATF4 (32,33).

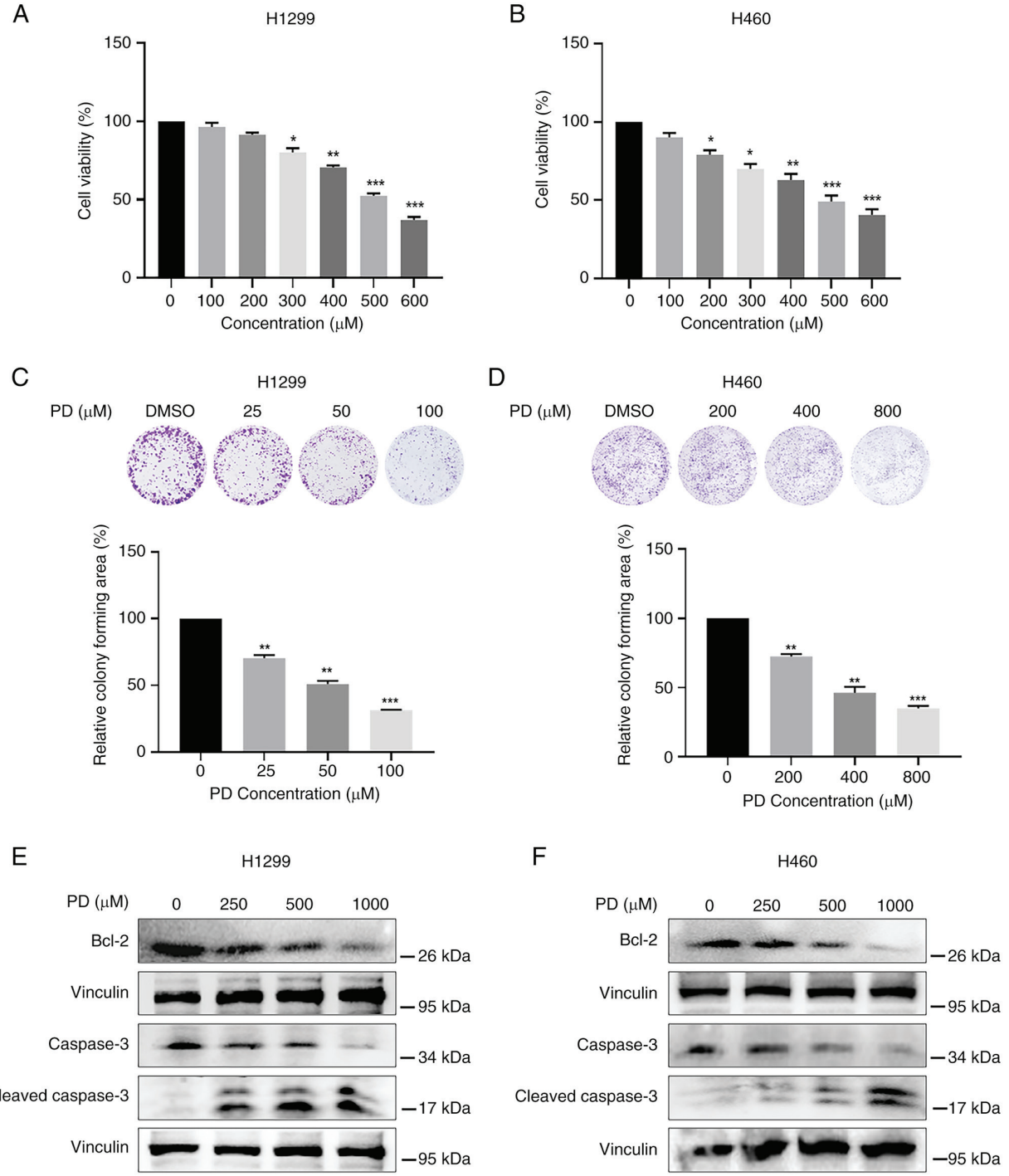

Figure 1. PD suppresses cell viability and colony formation, and promotes cell apoptosis in non-small cell lung cancer cells. (A) H1299 and (B) H460 cells were placed in a 96-well plate with various concentrations of PD (0-600 μM). After 72-h treatment with PD, MTT assay was employed to determine the cell viability. (C and D) Representative images of colony formation after PD treatment are shown in upper panel. (C) H1299 and (D) H460 cells were treated with various concentration of PD. The cells were stained with crystal violet after 7-10 days of treatment with PD. Quantification of colony formation data was conducted using ImageJ software. (E and F) Western blot analysis was performed to examine the expression levels of Bcl-2, Caspase3 and Cleaved-Caspase3 in (E) H1299 and (F) H460 cells following treatment with PD at indicated concentrations for 48 h. Vinculin was used as the internal control. Data were analyzed by using one-way ANOVA with Tukey's multiple comparisons test. Results are presented as the mean ± SD from three independent experiments. *P<0.05, **P<0.01 and ***P<0.001. PD, polydatin.

Treatment of both NSCLC cell lines (500 μM) with PD time-dependently elevated p-eIF2α and ATF4 expression levels (Fig. 2C and D). As expected, PD treatment dose-dependently elevated p-eIF2α and ATF4 expression levels in NSCLC cells (Fig. 2E and F), indicating that PD exerts antitumor effects in NSCLC cells by stimulating ROS-mediated ER stress pathway.

Cisplatin combined with PD exerts synergistic antitumor activities in NSCLC cells. To evaluate whether the combined treatment has superior anti-proliferative effects than mono-therapy, H1299 and H460 cells were treated with PD, cisplatin, or their combination. Treatment of NSCLC with varying doses of cisplatin inhibited cell viability of both H1299 and H460

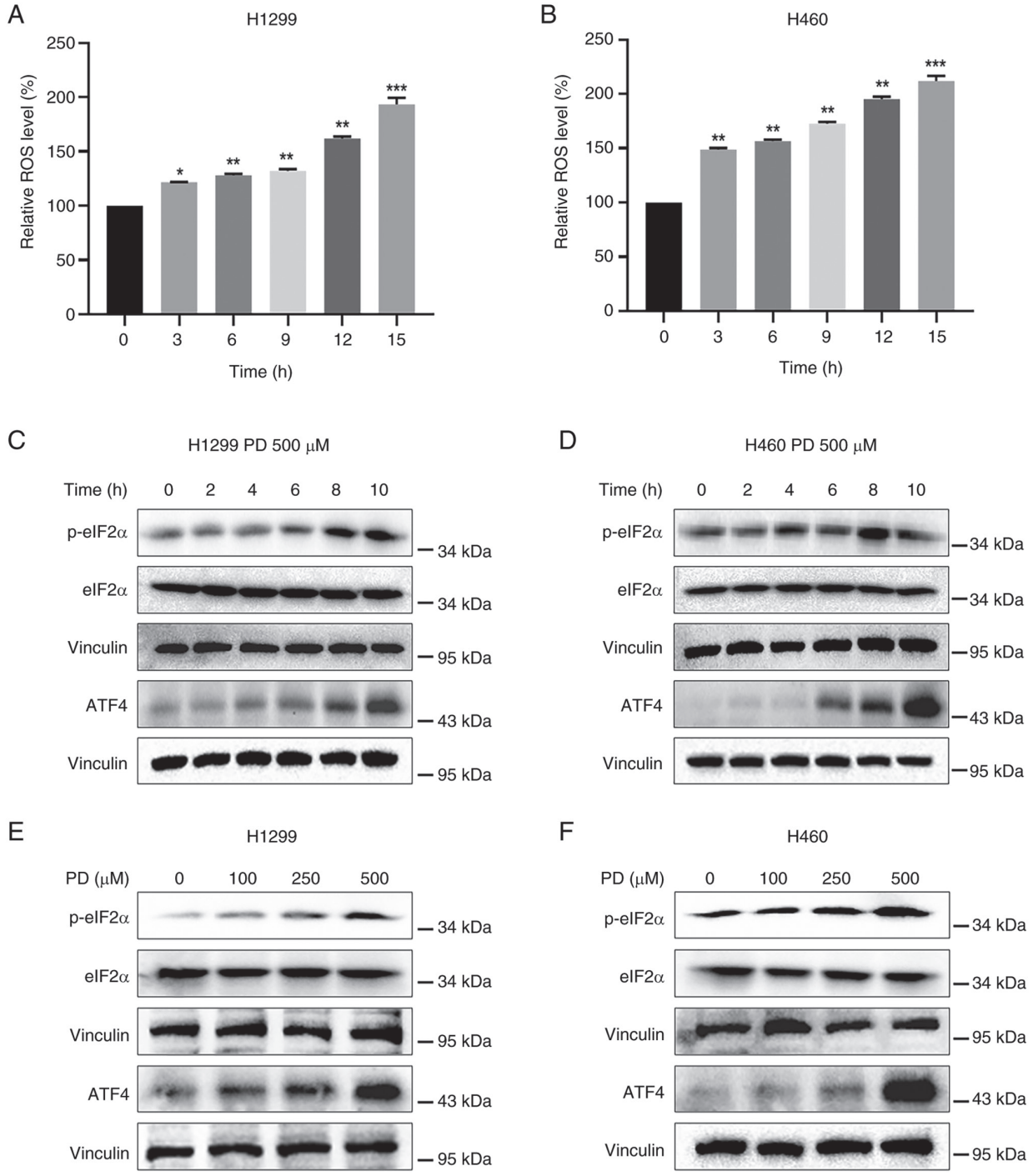

Figure 2. PD induces ER stress by promoting generation of ROS in non-small cell lung cancer cells. (A and B) Intracellular ROS generation was measured by DCFH-DA. (A) H1299 and (B) H460 cells were exposed to 500 μM PD for indicated time intervals and relative ROS levels were evaluated by fluorescent DCFH-DA probe. (C and D) PD led to increased generation of ROS and rapidly activated the ER stress pathway. (C) H1299 and (D) H460 cells were treated with 500 μM PD at indicated time points. The protein levels of p-eIF2α, eIF2α and ATF4 were detected by western blotting. Vinculin was used as the internal control. (E) H1299 and (F) H460 cells were exposed to various concentrations of PD for 8 h, and the protein levels of p-eIF2α, eIF2α and ATF4 were detected by western blotting. Vinculin was used as the internal control. Data were analyzed by using one-way ANOVA with Tukey's multiple comparisons test. Results are presented as the mean ± SD from three independent experiments. *P<0.05, **P<0.01 and ***P<0.001. PD, polydatin; ER, endoplasmic reticulum; ROS, reactive oxygen species; p-, phosphorylated.

cells in a dose-dependent manner. Additionally, 500 μM PD generally boosted cytotoxicity of cisplatin against H1299 cells, and robust synergistic inhibitory impact was observed in combined therapy with 60 μM cisplatin and 500 μM PD (Fig. 3A). In the same way, the application of 500 μM PD was found to augment cisplatin-induced cytotoxicity in H460 cells, and significant synergistic inhibitory effects were observed with combined therapy of 50 μM cisplatin and 500 μM PD (Fig. 3C). CompuSyn 2.0 software was utilized to calculate CI values assessing the interaction between PD and cisplatin. Notably, combinations of 60 μM cisplatin and 500 μM PD in H1299 cells (Fig. 3B) or 50 μM cisplatin and 500 μM PD in

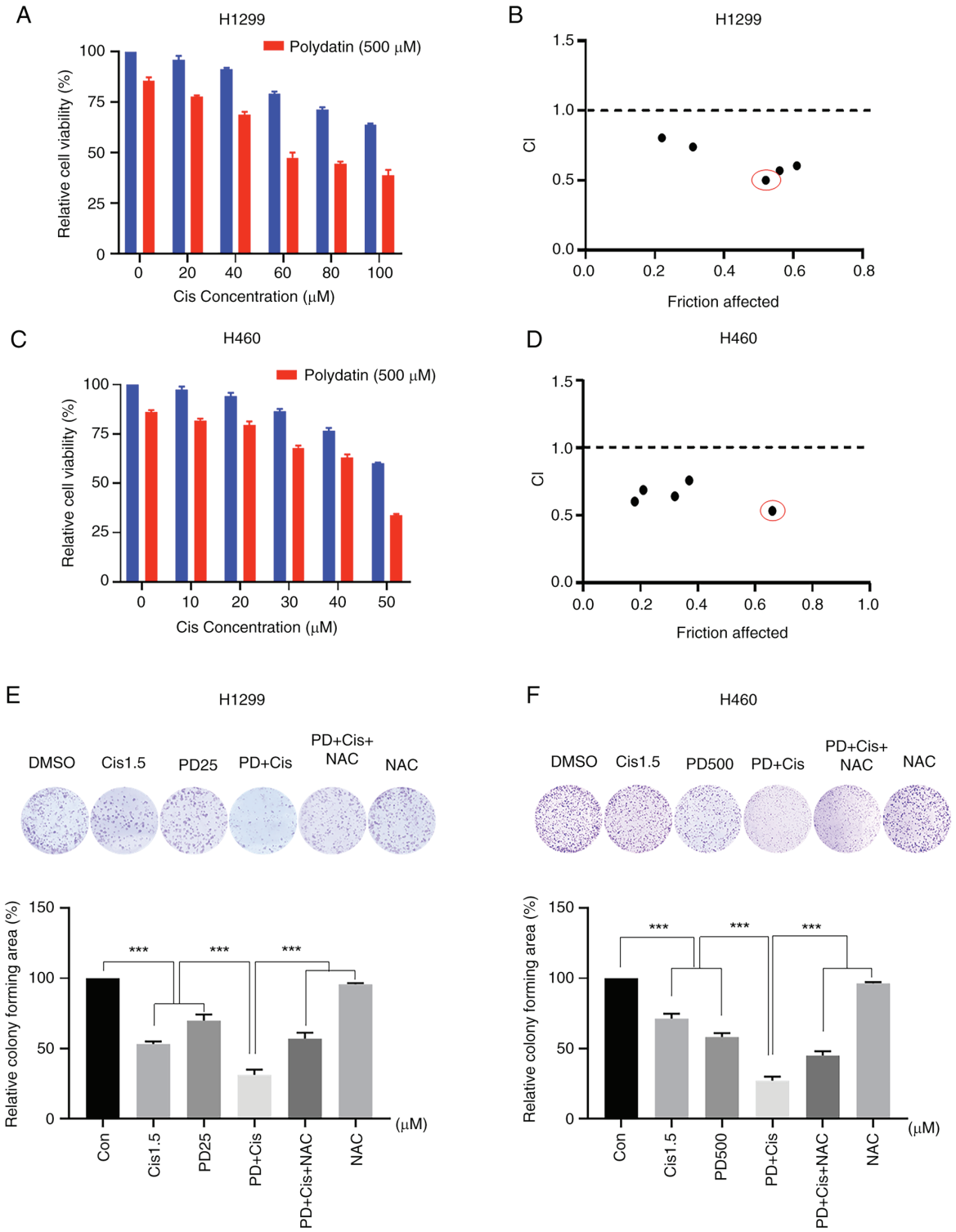

Figure 3. PD increases antitumor activity of cisplatin in non-small cell lung cancer cells. (A) H1299 (C) and H460 cells were treated with increasing doses of cisplatin (20-100 μM for H1299 cells and 10-50 μM for H460 cells) and PD (500 μM). The MTT assay was used to determine cell viability. (B and D) The Compusyn 2.0 software was employed to calculate the CI values for a range of fraction affected levels, which correspond to different levels of growth inhibition. Synergistic interaction was defined as CI values <1.0. (E) H1299 and (F) H460 cells were treated with PD, cisplatin or their combination. H1299 and H460 cells were pretreated with 5 mM NAC for 1.5 h prior to the combined treatment. Quantification of colony formation data was calculated by using ImageJ software. Data were analyzed by using one-way ANOVA with Tukey's multiple comparisons test. Results are presented as the mean ± SD from three independent experiments. ***P<0.001. PD, polydatin; CI, combination index; NAC, N-Acetyl-l-Cysteine.

H460 cells exhibited the lowest CI values amongst different combinations (Fig. 3D), indicating synergistic effects between PD and cisplatin in NSCLC. Furthermore, colony formation assay revealed that combined treatment of H1299 (25 μM) and H460 (500 μM) cells with PD and cisplatin (1.5 μM) significantly reduced colony forming ability of both cell lines when compared with single treatment alone (Fig. 3E and F). Importantly, combined treatment-induced inhibitory effects

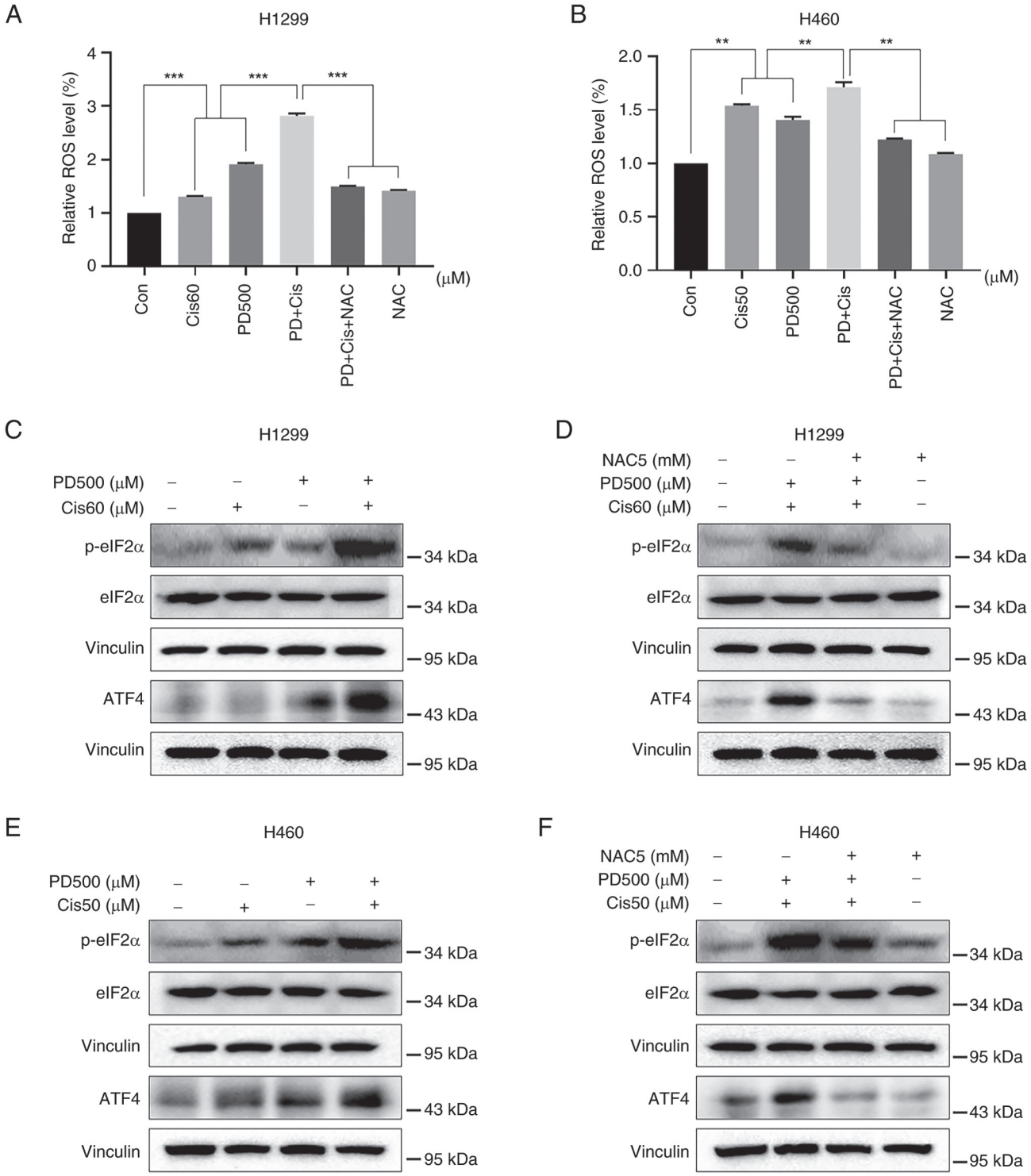

Figure 4. Combination of cisplatin and PD synergistically induces ROS-mediated endoplasmic reticulum stress in non-small cell lung cancer cells. (A) H1299 and (B) H460 cells were treated with cisplatin (60 μM for H1299 cells and 50 μM for H460 cells), PD (500 μM) or their combination. H1299 and H460 cells were pretreated with 5 mM NAC for 1.5 h before the combined treatment. The ROS levels were measured by fluorescent DCF-DA probe. Data were analyzed by using one-way ANOVA with Tukey's multiple comparisons test. Results are presented as the mean ± SD from three independent experiments. **P<0.01 and ***P<0.001. (C) H1299 and (E) H460 cells were treated with PD, cisplatin or their combination at the indicated doses. The protein levels of p-eIF2α, eIF2α and ATF4 were detected by western blot analysis. Vinculin was used as the internal control. (D) H1299 and (F) H460 cells were pretreated with NAC (5 mM) for 1.5 h before exposure to PD and cisplatin combination. The protein levels of p-eIF2α, eIF2α and ATF4 were evaluated by western blot analysis. Vinculin was used as the internal control. PD, polydatin; ROS, reactive oxygen species; NAC, N-Acetyl-l-Cysteine; p-, phosphorylated.

of colony forming ability were significantly attenuated by the ROS scavenger, NAC. Wound healing assay also showed similar results as combination of low dose of PD and cisplatin markedly inhibited the migration of NSCLC cells, and NAC pre-treatment effectively reversed this effect (Fig. S2). Similar with cisplatin, combination therapy with carboplatin and PD exhibited stronger inhibitory effects on H1299 and H460 cell viability (Fig. S3A-C) and colony formation (Fig. S3D-F)

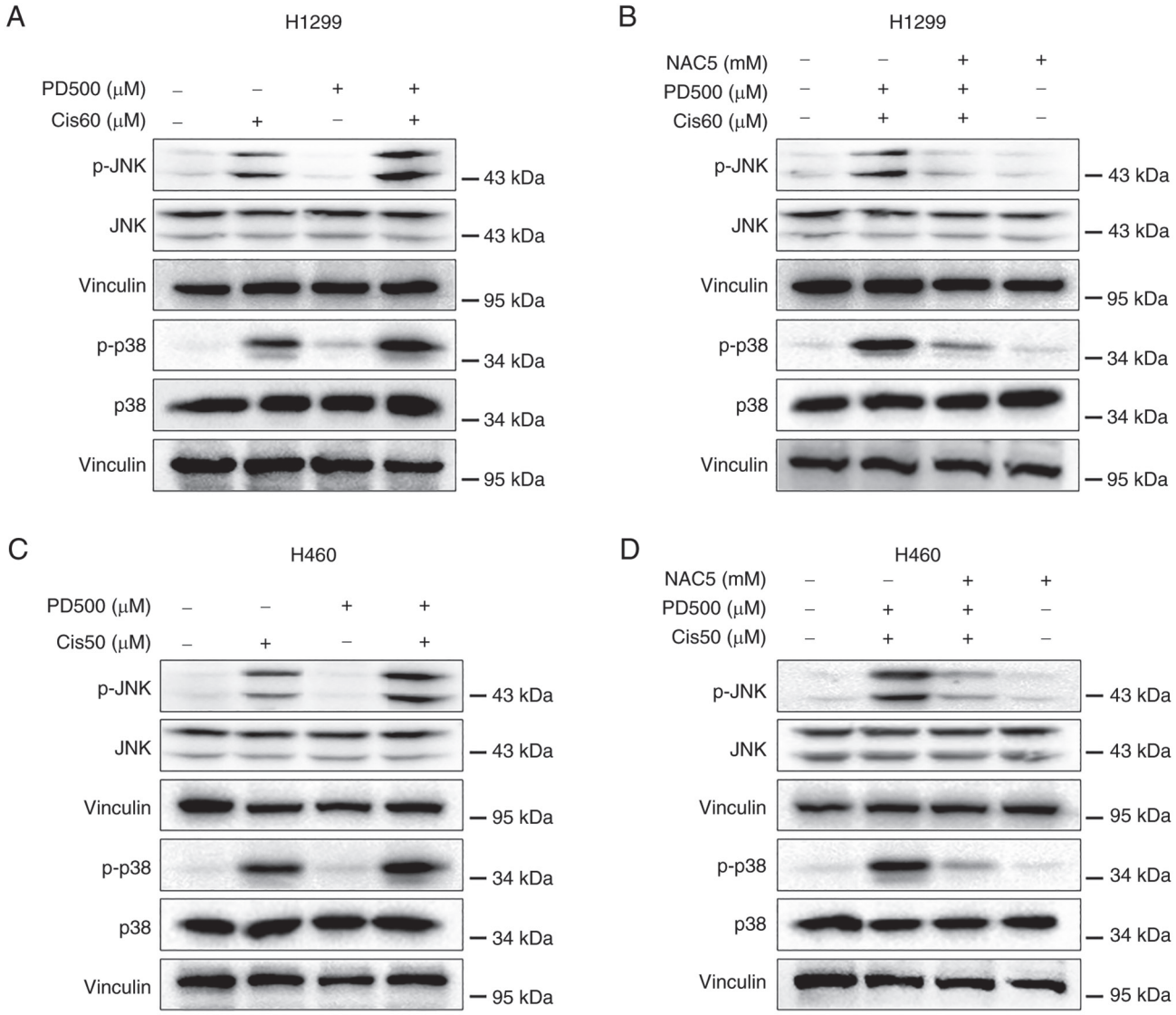

Figure 5. Combined treatment with PD and cisplatin activates reactive oxygen species-mediated JNK and p38 MAPK pathways in non-small cell lung cancer cells. (A) H1299 and (C) H460 cells were treated with PD, cisplatin or their combination at the indicated doses. After 8-h treatment, the protein levels of p-JNK, JNK, p-p38 and p38 were detected by western blot analysis. Vinculin was used as the internal control. (B) H1299 and (D) H460 cells were pretreated with NAC (5 mM) for 1.5 h before exposure to PD and cisplatin combination. After 8-h treatment, the protein levels of p-JNK, JNK, p-p38 and p38 were detected by western blot analysis. Vinculin was used as the internal control. PD, polydatin; NAC, N-Acetyl-l-Cysteine; p-, phosphorylated.

than single treatment alone. These findings indicated that a low dose of PD could improve antitumor effects of cisplatin and carboplatin, and that ROS is an important mediator in the synergistic effects of PD and cisplatin in NSCLC cells.

Combined treatment with PD and cisplatin stimulates ROS-mediated ER stress in NSCLC cells. Cancer cells have been observed to maintain higher levels of ROS compared with normal cells (34). This aspect provides an interesting therapeutic window since cancer cells might be more sensitive than normal cells to agents that induce ROS generation. In the present study, the intracellular ROS levels were examined in NSCLC cells after treatment with PD (500 μM), cisplatin (60 μM in H1299 cells and 50 μM in H460 cells), or combinations thereof. Combined treatment significantly induced generation of ROS when compared with PD or cisplatin alone, whilst NAC pre-treatment effectively prevented generation of ROS induced by combined treatments (Fig. 4A and B). ER stress-related proteins in cells were further investigated after treatment with PD, cisplatin, or their combination. Combined treatment markedly increased p-eIF2α and ATF4 expression in both H1299 and H460 cell lines, as compared with treatment with cisplatin or PD alone (Fig. 4C and E), whilst pre-treatment with NAC partly attenuated the expression of these ER stress-related proteins (Fig. 4D and F). These findings suggested that ROS-mediated ER stress functioned as a key role in the combined treatment, inducing synergistic antitumor activities in NSCLC cells.

Combined treatment of NSCLC cells with PD and cisplatin activates ROS-mediated JNK and p38 MAPK pathways. Apoptosis is tightly linked to the activated JNK and p38 MAPK pathways (35). Activation of the JNK and p38 pathways is closely involved in oxidative stress-induced apoptosis (36). Thus, the p-JNK and p38 protein levels were investigated in

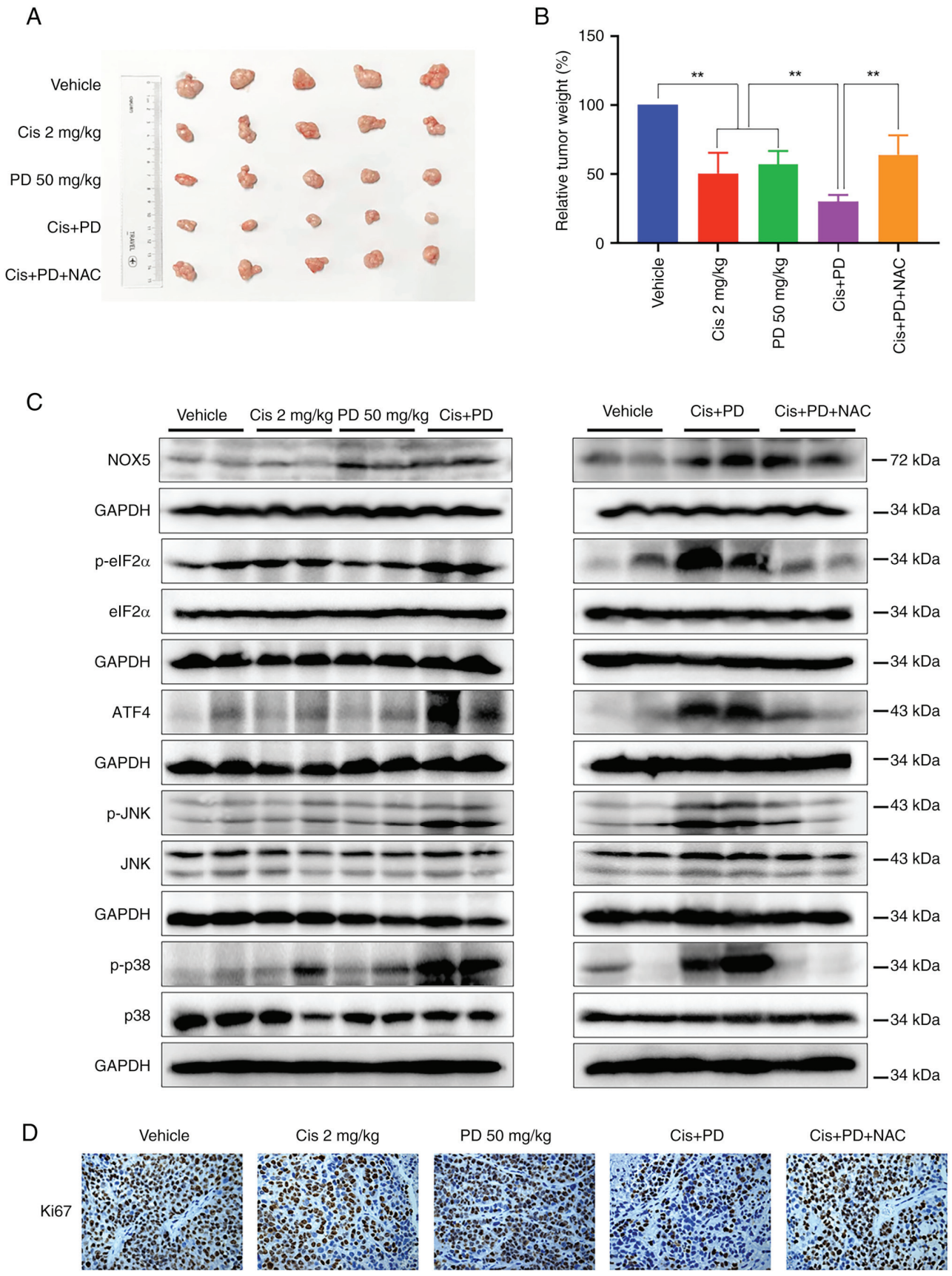

Figure 6. Combined treatment with PD and cisplatin synergistically inhibits tumor growth in mice xenograft models. (A and B) The tumor bearing mice were treated with PD (50 mg/kg), cisplatin (2 mg/kg) or their combination. The combined treatment significantly decreased (A) tumor volume and (B) weight, and NAC administration (0.5 g/l) reversed these effects. (C) The protein levels of NOX5, p-eIF2α, ATF4, p-p38, p-JNK and their corresponding total proteins in mice tumor specimens after treatment were determined by western blot analysis. GAPDH was used as the internal control. (D) The Ki-67 expression in tumor tissues was analyzed by immunohistochemical analysis (magnification, x200; scale bar, 50 μm). Data were analyzed by using one-way ANOVA with Tukey's multiple comparisons test. Results are presented as the mean ± SD from three independent experiments. **P<0.01. PD, polydatin; NAC, N-Acetyl-l-Cysteine; NOX5, NADPH oxidase 5; p-, phosphorylated.

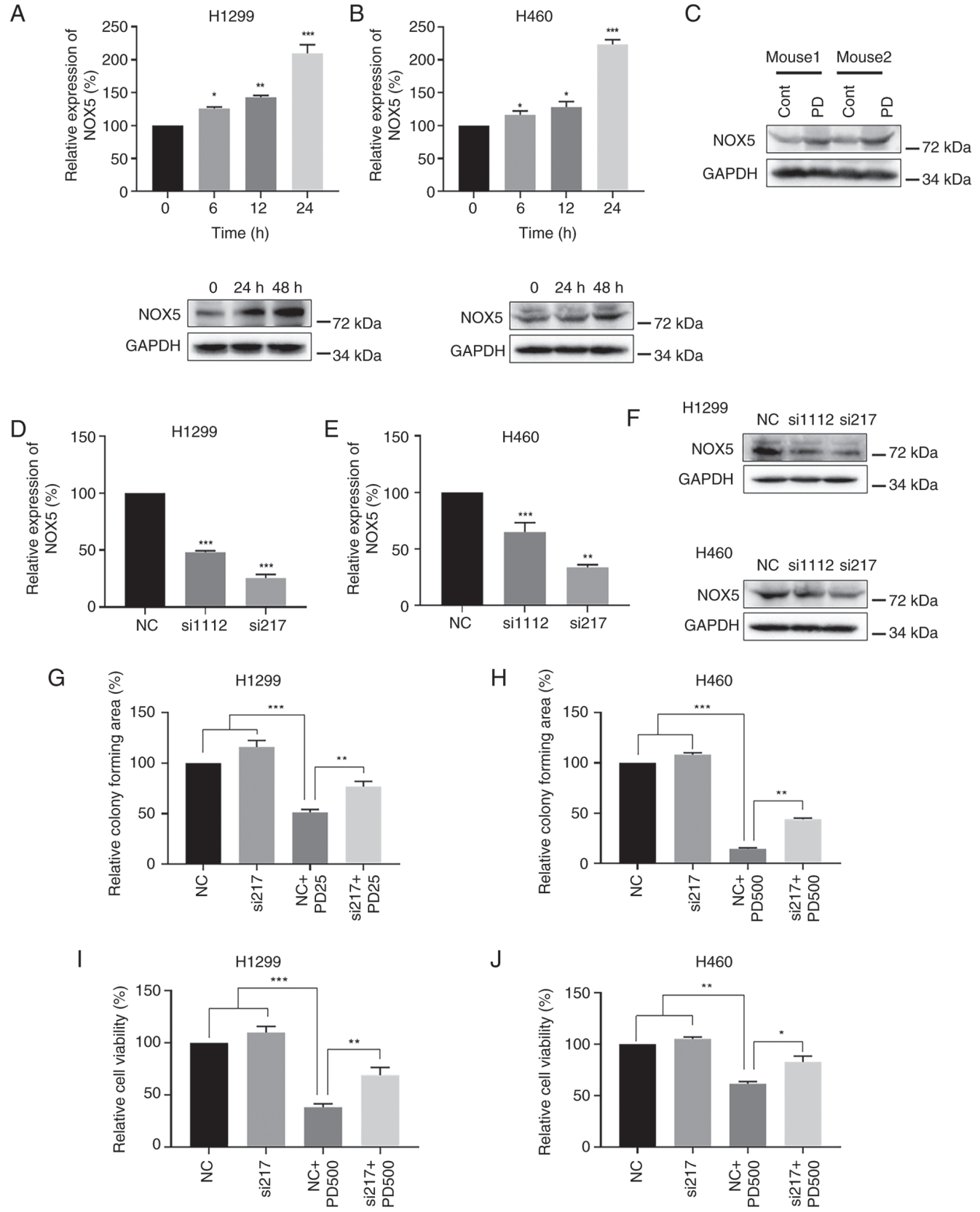

Figure 7. PD treatment increases expression of NOX5 in non-small cell lung cancer cells. (A) H1299 and (B) H460 cells were treated with PD, and NOX5 mRNA and protein expression levels were evaluated by RT-qPCR and western blot analyses, respectively. GAPDH was used as the internal control. (C) Western blot analysis detecting the expression levels of NOX5 protein in mice tumor tissues after treatment with PD. GAPDH was used as the internal control. (D-F) siRNAs against NOX5 were transfected into H1299 and H460 cells. (D and E) NOX5 mRNA and (F) protein levels were detected by RT-qPCR and western blot analyses, respectively. GAPDH was used as the internal control. (G) H1299 and (H) H460 cells were treated with PD (25 μM in H1299 cells and 500 μM in H460 cells), siNOX5 or their combination. Quantification of colony formation data was calculated by using ImageJ software. (I) H1299 and (J) H460 cells were treated with PD (500 μM), siNOX5 or their combination for 48 h. The cell viability was measured by MTT assay. Data were analyzed by using one-way ANOVA with Tukey's multiple comparisons test. Results are presented as the mean ± SD from three independent experiments. *P<0.05, **P<0.01 and ***P<0.001. PD, polydatin; NOX5, NADPH oxidase 5; RT-qPCR, reverse transcription-quantitative PCR; si-, small interfering; NC, negative control.

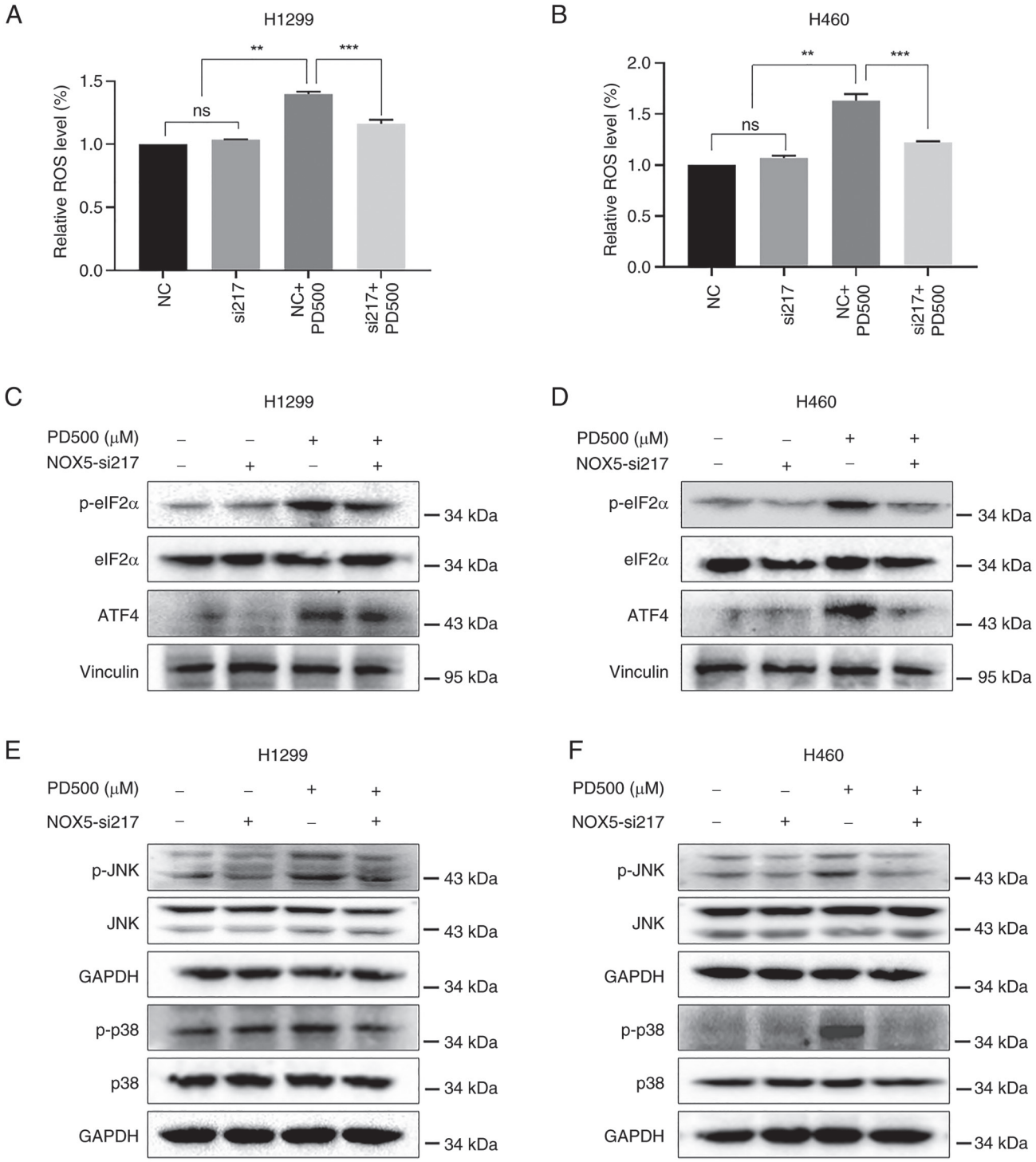

Figure 8. PD exerts antitumor activity in non-small cell lung cancer cells by stimulating NOX5-ROS-mediated endoplasmic reticulum-stress, and the JNK and p38 MAPK signaling pathways. (A) H1299 and (B) H460 cells were treated with siNOX5 for 18 h, and then treated with PD (500 μM) for 12 h. Relative ROS levels were evaluated by fluorescent DCF-DA probe. Data were analyzed by using one-way ANOVA with Tukey's multiple comparisons test. Results are presented as the mean ± SD from three independent experiments. **P<0.01 and ***P<0.001. (C-F) H1299 and H460 cells were pretreated with siNOX5 for 18 h before treatment with 500 μM PD. (C and D) After 6-h treatment, the protein levels of p-eIF2α, eIF2α, ATF4 were determined by western blot analysis. Vinculin was used as an internal control. (E and F) The protein levels of p-JNK, p-p38, JNK and p38 were detected by western blot analysis after 8-h PD treatment. GAPDH was used as an internal control. PD, polydatin; NOX5, NADPH oxidase 5; ROS, reactive oxygen species; si-, small interfering; p-, phosphorylated; ns, not significant (P>0.05).

H1299 and H460 cells following treatment with PD (500 μM), cisplatin (60 μM in H1299 cells or 50 μM in H460 cells), or their combination. Combined treatment of NSCLC cells with PD and cisplatin consistently elevated p-JNK and p38 expression (Fig. 5A and C), while pre-treatment with NAC effectively attenuated p-JNK and p-p38 levels induced by combined treatment (Fig. 5B and D). These results indicated that activation of ROS-mediated JNK and p38 MAPK signaling pathways contributed to the combined treatment, inducing synergistic antitumor activities.

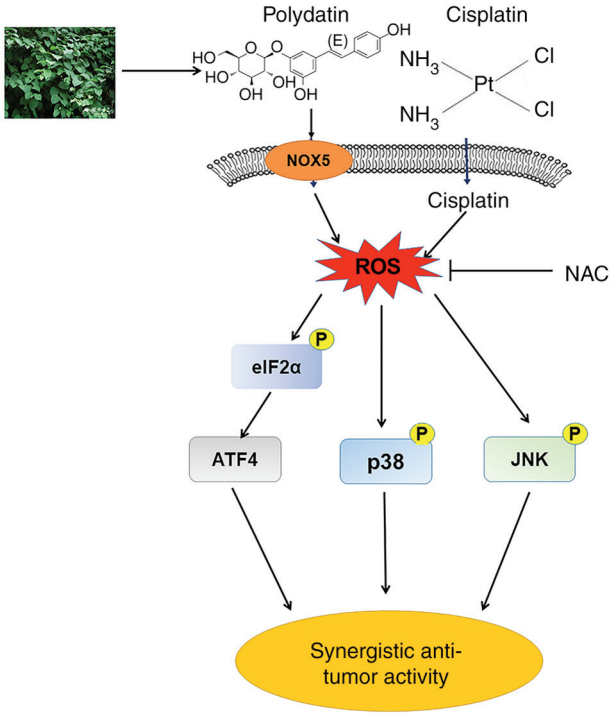

Figure 9. Schematic figure of the main findings of the present study. Polydatin potentiated antitumor activities of cisplatin by stimulating ER stress, and the JNK and p38 MAPK signaling pathways through promoting expression of NOX5. NOX5, NADPH oxidase 5; ROS, reactive oxygen species.

Combined treatment with PD and cisplatin exhibits synergistic antitumor activity in mice xenograft models. To further investigate the synergistic antitumor effects of combined treatment with PD and cisplatin on NSCLC *in vivo*, H460 xenografts were established in nude mice. The mice were divided into five experimental groups (n=5), and were administered 2 mg/kg cisplatin every three days, 50 mg/kg PD every two days, or their combination for two weeks. The combined treatment group was further divided into two sub-groups, with one sub-group administered NAC in their drinking water (0.5 g/l). The results showed that the combined treatment significantly inhibited tumor growth *in vivo* compared with cisplatin or PD treatment alone, while this inhibitory effect was reversed in the NAC treatment sub-group (Figs. 6A and B and S4A). There were no notable differences in body weight changes between the combined treatment group and the other groups (Fig. S4B). Additionally, H&E staining demonstrated no histological alterations in vital organs (heart, lung, kidney and liver) (Fig. S4C), suggesting that the combined treatment was administered at rational drug doses and did not induce any significant cytotoxicity in the experimental subjects. Similar with *in vitro* results, the expression levels of p-eIF2α, ATF4, p-JNK and p-p38 in tumor tissues exhibited a marked increase in the combined treatment group as compared with single treatment groups. Moreover, pre-treatment with NAC consistently attenuated the increase of these proteins in tumor tissues from the combined treatment group (Fig. 6C). As expected, PD treatment increased NOX5 protein expression, whereas cisplatin did not, suggesting that cisplatin increases ROS levels through a NOX5-independent pathway. Accordingly, the combination of cisplatin and PD did not markedly increase NOX5 protein levels compared with PD treatment alone. Additionally, NAC pre-treatment did not reverse the combination treatment-induced NOX5 protein levels, indicating that ROS may not be upstream of NOX5. Furthermore, the IHC staining analysis demonstrated that the co-administration of cisplatin and PD resulted in a significant reduction of Ki-67 positive cells. Notably, the pre-treatment with NAC reversed the aforementioned effects induced by the combined treatment (Fig. 6D). These findings suggested that PD enhanced the antitumor activities of cisplatin *in vivo* at least partly by stimulating ROS-mediated ER stress, JNK and p38 MAPK signaling pathways.

PD exerts antitumor activities by targeting NOX5 in NSCLC cells. NOX5 activation stimulates production of ROS and causes subsequent death of tumor cells (24,37,38). It was found that PD treatment increased generation of ROS in NSCLC cells. Thus, it was hypothesized that PD might promote NOX5 activity to regulate generation of ROS. Treatment of NSCLC cells with PD significantly increased both NOX5 mRNA and protein expression levels (Fig. 7A and B). Similarly, PD treatment consistently upregulated NOX5 protein expression in mouse xenograft tumor tissues (Fig. 7C). To further evaluate the impact of NOX5 in PD-induced generation of ROS, NOX5 was knocked down by two independent siRNAs. Knocking down NOX5 consistently reduced both NOX5 mRNA (Fig. 7D and E) and protein expression levels in H1299 and H460 NSCLC cells (Fig. 7F). Since si-217 exhibited stronger knockdown effect than si-1112, si-217 was used for further analyses. Additionally, knocking down NOX5 attenuated the inhibitory effects of PD on NSCLC colony formation (Figs. 7G and H; S5C and D) and cell viability (Figs. 7I and J; S5A and B). Furthermore, knocking down NOX5 reduced PD-induced production of ROS in NSCLC cells (Fig. 8A and B). Additionally, knocking down NOX5 partly diminished PD-induced activation of ER stress-related proteins (p-eIF2α and ATF4) (Fig. 8C and D), and the JNK and p38 MAPK pathways (Fig. 8E and F). These results indicated that NOX5 is a possible target of PD and an important mediator of PD-induced cell death in NSCLC cells.

Discussion

Despite recent advancements in understanding the molecular, pathological and biological aspect of NSCLC, it remains a devastating disease with limited options for effective treatments (39). Additionally, the main obstacle of chemotherapy and targeted therapy is inevitable drug resistance (40). Cisplatin-based chemotherapies were widely recognized as the standard treatment regimen for numerous types of cancers, including NSCLC. However, emergence of drug resistance and systemic cytotoxicity limited its application (41).

A number of studies have reported that natural products exert prominent antitumor activity by increasing generation of ROS. Isoalantolactone inhibited prostate cancer cell proliferation by inducing production of ROS, activating ER stress and inhibiting the STAT3 signaling pathways (42). Celastrol, a *Tripterygium wilfordii* extract, exerted anti-NSCLC activities

by increasing generation of ROS, disrupting mitochondrial membrane potential, and promoting mitochondrial fission (43). Accumulating evidences have suggested that combined treatment with natural products and cisplatin exerted synergetic antitumor activities (44,45). Thus, combined therapeutic strategies with natural products and chemotherapeutic agents might overcome drug resistance and minimize cytotoxicity.

In the present study, the unrecognized role of PD in NSCLC was comprehensively analyzed. It was found for the first time, to the best of our knowledge, that PD stimulated ROS-mediated ER stress by targeting NOX5, thereby exerting antitumor activity in NSCLC. Furthermore, it was revealed that the combination of PD and cisplatin synergistically enhanced anti-NSCLC activity through the activation of ROS-mediated ER stress, and the JNK and p38 MAPK signaling pathways (Fig. 9). These results highlight the potential therapeutic implications of PD in NSCLC and provide novel insights suggesting that combination therapy involving PD and cisplatin may be a promising approach for the treatment of NSCLC.

PD, a small natural compound from *Polygonum cuspidatum*, exerts prominent antitumor activities in various cancers by inducing apoptosis (27-29). PD inhibited nasopharyngeal carcinoma cell proliferation by inhibiting ROS-mediated Akt signaling and triggering ER stress-mediated apoptotic pathways (30). PD has also been reported to inhibit Nrf2 protein expression and promote generation of ROS in triple-negative breast cancer cells (46). Additionally, PD decreased the mitochondrial membrane potential and increased generation of ROS, resulting in inducing leukemia cell apoptosis and cell cycle arrest (47). However, underlying molecular mechanisms of PD and its effects on cisplatin-mediated antitumor activity in NSCLC are unclear. In the present study, it was found that PD synergistically enhanced antitumor activity of cisplatin in NSCLC by promoting generation of ROS. Importantly, treatment of normal human cells with high dose of PD showed only minor cytotoxicity when compared with NSCLC cells, suggesting high druggable potential of PD in NSCLC. Increased production of ROS induces abnormal unfolded protein expression in the ER, and triggers the ER stress response (32). Additionally, Protein kinase R (PKR)-like ER kinase (PERK)-mediated p-eIF2α-ATF4 pathway activation was frequently observed under ER stress (33). It was demonstrated that combined treatment with PD and cisplatin markedly increased the expression of ER stress-related proteins (ATF4 and p-eIF2α), as compared with single treatment alone. Moreover, pre-treatment with NAC effectively attenuated these effects. These results suggested that PD potentiates antitumor activities of cisplatin by partly stimulating ROS-mediated ER stress.

Accumulating evidences have shown that ROS-mediated activation of JNK and p38 MAPK pathways promoted cell apoptosis (36,48). Nevertheless, association between the JNK/p38 MAPK signaling pathways and PD induced cell death, and underlying molecular mechanisms of combined treatment with PD and cisplatin in NSCLC are largely unknown. The present study demonstrated that combined treatment consistently increased p-JNK and p-p38 expression levels by promoting ROS production both *in vitro* and *in vivo*, suggesting that ROS-mediated ER stress, and the JNK and p38 MAPK pathways contributed to the synergistic antitumor activity of combined treatment with PD and cisplatin in NSCLC.

It has been demonstrated that PD treatment consistently induces generation of ROS in NSCLC cells. However, direct target of PD and its underlying molecular mechanisms remain elusive. NOX5, a member of NOXs, plays critical role in regulating the redox balance in cells. Accumulating evidences suggested that NOX5 activation is closely involved in production of intracellular ROS (49,50). NOX5 acts as a either tumor suppressor or oncogene in a context-dependent manner (24,49). In esophageal squamous cell carcinoma (ESCC), Src-mediated NOX5 activation was correlated to the poor prognosis of ESCC (49). Inversely, DHTS-induced activation of NOX5 inhibited proliferation of breast CSCs by inhibiting the ROS-mediated STAT3 pathway (24). However, no studies have reported the association between PD and NOX5 on production of ROS in cancer cells. In the present study, it was demonstrated for the first time to the best of our knowledge, that PD exerted antitumor activity by promoting expression of NOX5 and subsequent generation of ROS. Additionally, knockdown of NOX5 significantly attenuated the antitumor activity of PD and its effects on the activation of ER stress and the MAPK pathways by inhibiting production of ROS. These findings suggested a pivotal role of NOX5 in PD-mediated NSCLC cell death. However, the detailed regulatory mechanisms of PD on the JNK and p38 MAPK pathways require further elucidation.

In conclusion, PD enhanced the antitumor activities of cisplatin in NSCLC by activating ROS-mediated ER stress, and the JNK and p38 MAPK pathways. Mechanistically, PD promoted generation of ROS in NSCLC cells by inducing expression of NOX5. The present study indicated that the combined therapy with PD and cisplatin might be an effective therapeutic strategy for some patients with NSCLC.

Acknowledgements

Not applicable.

Funding

The present study was supported by the National Natural Science Foundation of China (grant no. 81672305), the Health Commission of Zhejiang (grant no. 2022RC292) and the Natural Science Foundation of Zhejiang (grant no. LZ22H160006).

Availability of data and materials

The data generated in the present study may be requested from the corresponding author.

Authors' contributions

RC conceived the study and designed the research. SW, QZ, SL, JK, JZ, AO and YS performed the *in vitro* experiments. SW, QZ, JW, HS, LN, YY and XT performed mice xenograft experiments. SW and QZ contributed to the data acquisition. WZ, YZ and HL analyzed the data. RC, WZ and SW wrote and edited the manuscript. RC and WZ supervised the research. All authors read and approved the final manuscript. SW, QZ and WZ confirm the authenticity of all the raw data.

Ethics approval and consent to participate

All animal experiments were carried out in accordance with the Wenzhou Medical University's Institutional Animal Care and Use Committee (IACUC) guidelines (approval no. xmsq2022-0602; Wenzhou, China).

Patient consent for publication

Not applicable.

Competing interests

The authors declare that they have no competing interests.

References

1. Jemal A, Bray F, Center MM, Ferlay J, Ward E and Forman D: Global cancer statistics. CA Cancer J Clin 61: 69-90, 2011.
2. Ettinger DS, Akerley W, Borghaei H, Chang AC, Cheney RT, Chirieac LR, D'Amico TA, Demmy TL, Ganti AK, Govindan R, *et al*: Non-small cell lung cancer. J Natl Compr Canc Netw 10: 1236-1271, 2012.
3. Zarogoulidis K, Zarogoulidis P, Darwiche K, Boutsikou E, Machairiotis N, Tsakiridis K, Katsikogiannis N, Kougioumtzi I, Karapantzos I, Huang H and Spyratos D: Treatment of non-small cell lung cancer (NSCLC). J Thorac Dis 5 (Suppl 4): S389-S396, 2013.
4. Chen W, Zheng R, Baade PD, Zhang S, Zeng H, Bray F, Jemal A, Yu XQ and He J: Cancer statistics in China, 2015. CA Cancer J Clin 66: 115-132, 2016.
5. Bunn PA Jr: The expanding role of cisplatin in the treatment of non-small-cell lung cancer. Semin Oncol 16 (4 Suppl 6): S10-S21, 1989.
6. Minami D, Takigawa N, Takeda H, Takata M, Ochi N, Ichihara E, Hisamoto A, Hotta K, Tanimoto M and Kiura K: Synergistic effect of olaparib with combination of cisplatin on PTEN-deficient lung cancer cells. Mol Cancer Res 11: 140-148, 2013.
7. Cui Z, Li D, Zhao J and Chen K: Falnidamol and cisplatin combinational treatment inhibits non-small cell lung cancer (NSCLC) by targeting DUSP26-mediated signal pathways. Free Radic Biol Med 183: 106-124, 2022.
8. Han Y, Shi J, Xu Z, Zhang Y, Cao X, Yu J, Li J and Xu S: Identification of solamargine as a cisplatin sensitizer through phenotypical screening in cisplatin-resistant NSCLC organoids. Front Pharmacol 13: 802168, 2022.
9. Li H, Zhu X, Zhang Y, Xiang J and Chen H: Arsenic trioxide exerts synergistic effects with cisplatin on non-small cell lung cancer cells via apoptosis induction. J Exp Clin Cancer Res 28: 110, 2009.
10. Xue DF, Pan ST, Huang G and Qiu JX: ROS enhances the cytotoxicity of cisplatin by inducing apoptosis and autophagy in tongue squamous cell carcinoma cells. Int J Biochem Cell Biol 122: 105732, 2020.
11. Kleih M, Böpple K, Dong M, Gaißler A, Heine S, Olayioye MA, Aulitzky WE and Essmann F: Direct impact of cisplatin on mitochondria induces ROS production that dictates cell fate of ovarian cancer cells. Cell Death Dis 10: 851, 2019.
12. McWhinney SR, Goldberg RM and McLeod HL: Platinum neurotoxicity pharmacogenetics. Mol Cancer Ther 8: 10-16, 2009.
13. Liu Y, Song Z, Liu Y, Ma X, Wang W, Ke Y, Xu Y, Yu D and Liu H: Identification of ferroptosis as a novel mechanism for antitumor activity of natural product derivative a2 in gastric cancer. Acta Pharm Sin B 11: 1513-1525, 2021.
14. Jin J, Qiu S, Wang P, Liang X, Huang F, Wu H, Zhang B, Zhang W, Tian X, Xu R, *et al*: Cardamonin inhibits breast cancer growth by repressing HIF-1α-dependent metabolic reprogramming. J Exp Clin Cancer Res 38: 377, 2019.
15. Wang L, Wang C, Tao Z, Zhao L, Zhu Z, Wu W, He Y, Chen H, Zheng B, Huang X, *et al*: Curcumin derivative WZ35 inhibits tumor cell growth via ROS-YAP-JNK signaling pathway in breast cancer. J Exp Clin Cancer Res 38: 460, 2019.
16. Yu Y, Chen D, Wu T, Lin H, Ni L, Sui H, Xiao S, Wang C, Jiang S, Pan H, *et al*: Dihydroartemisinin enhances the anti-tumor activity of oxaliplatin in colorectal cancer cells by altering PRDX2-reactive oxygen species-mediated multiple signaling pathways. Phytomedicine 98: 153932, 2022.
17. Ye J, Piao H, Jiang J, Jin G, Zheng M, Yang J, Jin X, Sun T, Choi YH, Li L and Yan G: Polydatin inhibits mast cell-mediated allergic inflammation by targeting PI3K/Akt, MAPK, NF-κB and Nrf2/HO-1 pathways. Sci Rep 7: 11895, 2017.
18. Hogg SJ, Chitcholtan K, Hassan W, Sykes PH and Garrill A: Resveratrol, acetyl-resveratrol, and polydatin exhibit antigrowth activity against 3D cell aggregates of the SKOV-3 and OVCAR-8 ovarian cancer cell lines. Obstet Gynecol Int 2015: 279591, 2015.
19. Chen S, Tao J, Zhong F, Jiao Y, Xu J, Shen Q, Wang H, Fan S and Zhang Y: Polydatin down-regulates the phosphorylation level of Creb and induces apoptosis in human breast cancer cell. PLoS One 12: e0176501, 2017.
20. Jiang CQ, Ma LL, Lv ZD, Feng F, Chen Z and Liu ZD: Polydatin induces apoptosis and autophagy via STAT3 signaling in human osteosarcoma MG-63 cells. J Nat Med 74: 533-544, 2020.
21. Zhao W, Chen Z and Guan M: Polydatin enhances the chemosensitivity of osteosarcoma cells to paclitaxel. J Cell Biochem 120: 17481-17490, 2019.
22. Quagliariello V, Berretta M, Buccolo S, Iovine M, Paccone A, Cavalcanti E, Taibi R, Montopoli M, Botti G and Maurea N: Polydatin reduces cardiotoxicity and enhances the anticancer effects of sunitinib by decreasing pro-oxidative stress, pro-inflammatory cytokines, and NLRP3 inflammasome expression. Front Oncol 11: 680758, 2021.
23. Bedard K and Krause KH: The NOX family of ROS-generating NADPH oxidases: Physiology and pathophysiology. Physiol Rev 87: 245-313, 2007.
24. Kim SL, Choi HS, Kim JH, Jeong DK, Kim KS and Lee DS: Dihydrotanshinone-induced NOX5 activation inhibits breast cancer stem cell through the ROS/Stat3 signaling pathway. Oxid Med Cell Longev 2019: 9296439, 2019.
25. Huang Z, Su Q, Li W, Ren H, Huang H and Wang A: Suppressed mitochondrial respiration via NOX5-mediated redox imbalance contributes to the antitumor activity of anlotinib in oral squamous cell carcinoma. J Genet Genomics 48: 582-594, 2021.
26. Livak KJ and Schmittgen TD: Analysis of relative gene expression data using real-time quantitative PCR and the 2(-Delta Delta C(T)) method. Methods 25: 402-408, 2001.
27. Bae H, Lee W, Song J, Hong T, Kim MH, Ham J, Song G and Lim W: Polydatin counteracts 5-fluorouracil resistance by enhancing apoptosis via calcium influx in colon cancer. Antioxidants (Basel) 10: 1477, 2021.
28. Bai L, Ma Y, Wang X, Feng Q, Zhang Z, Wang S, Zhang H, Lu X, Xu Y, Zhao E and Cui H: Polydatin inhibits cell viability, migration, and invasion through suppressing the c-Myc expression in human cervical cancer. Front Cell Dev Biol 9: 587218, 2021.
29. Bang TH, Park BS, Kang HM, Kim JH and Kim IR: Polydatin, a glycoside of resveratrol, induces apoptosis and inhibits metastasis oral squamous cell carcinoma cells in vitro. Pharmaceuticals (Basel) 14: 902, 2021.
30. Liu H, Zhao S, Zhang Y, Wu J, Peng H, Fan J and Liao J: Reactive oxygen species-mediated endoplasmic reticulum stress and mitochondrial dysfunction contribute to polydatin-induced apoptosis in human nasopharyngeal carcinoma CNE cells. J Cell Biochem 112: 3695-3703, 2011.
31. Moloney JN and Cotter TG: ROS signalling in the biology of cancer. Semin Cell Dev Biol 80: 50-64, 2018.
32. Verfaillie T, Rubio N, Garg AD, Bultynck G, Rizzuto R, Decuypere JP, Piette J, Linehan C, Gupta S, Samali A and Agostinis P: PERK is required at the ER-mitochondrial contact sites to convey apoptosis after ROS-based ER stress. Cell Death Differ 19: 1880-1891, 2012.
33. Balsa E, Soustek MS, Thomas A, Cogliati S, García-Poyatos C, Martín-García E, Jedrychowski M, Gygi SP, Enriquez JA and Puigserver P: ER and nutrient stress promote assembly of respiratory chain supercomplexes through the PERK-eIF2α axis. Mol Cell 74: 877-890.e6, 2019.
34. Trachootham D, Alexandre J and Huang P: Targeting cancer cells by ROS-mediated mechanisms: A radical therapeutic approach? Nat Rev Drug Discov 8: 579-591, 2009.
35. Sui X, Kong N, Ye L, Han W, Zhou J, Zhang Q, He C and Pan H: p38 and JNK MAPK pathways control the balance of apoptosis and autophagy in response to chemotherapeutic agents. Cancer Lett 344: 174-179, 2014.

36. Kwak AW, Lee MJ, Lee MH, Yoon G, Cho SS, Chae JI and Shim JH: The 3-deoxysappanchalcone induces ROS-mediated apoptosis and cell cycle arrest via JNK/p38 MAPKs signaling pathway in human esophageal cancer cells. Phytomedicine 86: 153564, 2021.
37. Huang WC, Li X, Liu J, Lin J and Chung LWK: Activation of androgen receptor, lipogenesis, and oxidative stress converged by SREBP-1 is responsible for regulating growth and progression of prostate cancer cells. Mol Cancer Res 10: 133-142, 2012.
38. Park S, Oh SS, Lee KW, Lee YK, Kim NY, Kim JH, Yoo J and Kim KD: NDRG2 contributes to cisplatin sensitivity through modulation of BAK-to-Mcl-1 ratio. Cell Death Dis 9: 30, 2018.
39. Brahmer J, Reckamp KL, Baas P, Crinò L, Eberhardt WE, Poddubskaya E, Antonia S, Pluzanski A, Vokes EE, Holgado E, *et al*: Nivolumab versus Docetaxel in advanced squamous-cell non-small-cell lung cancer. N Engl J Med 373: 123-135, 2015.
40. Rotow J and Bivona TG: Understanding and targeting resistance mechanisms in NSCLC. Nat Rev Cancer 17: 637-658, 2017.
41. Fennell DA, Summers Y, Cadranel J, Benepal T, Christoph DC, Lal R, Das M, Maxwell F, Visseren-Grul C and Ferry D: Cisplatin in the modern era: The backbone of first-line chemotherapy for non-small cell lung cancer. Cancer Treat Rev 44: 42-50, 2016.
42. Chen W, Li P, Liu Y, Yang Y, Ye X, Zhang F and Huang H: Isoalantolactone induces apoptosis through ROS-mediated ER stress and inhibition of STAT3 in prostate cancer cells. J Exp Clin Cancer Res 37: 309, 2018.
43. Liu M, Fan Y, Li D, Han B, Meng Y, Chen F, Liu T, Song Z, Han Y, Huang L, *et al*: Ferroptosis inducer erastin sensitizes NSCLC cells to celastrol through activation of the ROS-mitochondrial fission-mitophagy axis. Mol Oncol 15: 2084-2105, 2021.
44. Sioud F, Amor S, Toumia IB, Lahmar A, Aires V, Chekir-Ghedira L and Delmas D: A new highlight of Ephedra alata decne properties as potential adjuvant in combination with cisplatin to induce cell death of 4t1 breast cancer cells in vitro and in vivo. Cells 9: 362, 2020.
45. Araújo RF Jr, Soares LA, da Costa Porto CR, de Aquino RG, Guedes HG, Petrovick PR, de Souza TP, Araújo AA and Guerra GC: Growth inhibitory effects of Phyllanthus niruri extracts in combination with cisplatin on cancer cell lines. World J Gastroenterol 18: 4162-6168, 2012.
46. Li J, Zhang J, Zhu Y, Afolabi LO, Chen L and Feng X: Natural compounds, optimal combination of brusatol and polydatin promote anti-tumor effect in breast cancer by targeting Nrf2 signaling pathway. Int J Mol Sci 24: 8265, 2023.
47. Cao WJ, Wu K, Wang C and Wan DM: Polydatin-induced cell apoptosis and cell cycle arrest are potentiated by Janus kinase 2 inhibition in leukemia cells. Mol Med Rep 13: 3297-3302, 2016.
48. Cao X, Fu M, Bi R, Zheng X, Fu B, Tian S, Liu C, Li Q and Liu J: Cadmium induced BEAS-2B cells apoptosis and mitochondria damage via MAPK signaling pathway. Chemosphere 263: 128346, 2021.
49. Chen J, Wang Y, Zhang W, Zhao D, Zhang L, Fan J, Li J and Zhan Q: Membranous NOX5-derived ROS oxidizes and activates local Src to promote malignancy of tumor cells. Signal Transduct Target Ther 5: 139, 2020.
50. da Silva JF, Alves JV, Silva-Neto JA, Costa RM, Neves KB, Alves-Lopes R, Carmargo LL, Rios FJ, Montezano AC, Touyz RM and Tostes RC: Lysophosphatidylcholine induces oxidative stress in human endothelial cells via NOX5 activation-implications in atherosclerosis. Clin Sci (Lond) 135: 1845-1858, 2021.